Hindawi
Advances in High Energy Physics
Volume 2019, Article ID 1287932, 9 pages
https://doi.org/10.1155/2019/1287932

*Research Article*

# Cosmological Implications of the Generalized Entropy Based Holographic Dark Energy Models in Dynamical Chern-Simons Modified Gravity

**M. Younas,[1] Abdul Jawad ,[1] Saba Qummer,[1] H. Moradpour ,[2] and Shamaila Rani [1]**

[1] *Department of Mathematics, COMSATS University Islamabad, Lahore Campus-54000, Pakistan*
[2] *Research Institute for Astronomy and Astrophysics of Maragha (RIAAM), P.O. Box 55134-441, Maragha, Iran*

Correspondence should be addressed to Abdul Jawad; abduljawad@cuilahore.edu.pk

Received 28 August 2018; Revised 8 November 2018; Accepted 5 December 2018; Published 8 January 2019

Academic Editor: Chao-Qiang Geng



Recently, Tsallis, Rényi, and Sharma-Mittal entropies have widely been used to study the gravitational and cosmological setups. We consider a flat FRW universe with linear interaction between dark energy and dark matter. We discuss the dark energy models using Tsallis, Rényi, and Sharma-Mittal entropies in the framework of Chern-Simons modified gravity. We explore various cosmological parameters (equation of state parameter, squared sound of speed ) and cosmological plane ($\omega_d - \omega_d'$, where $\omega_d'$ is the evolutionary equation of state parameter). It is observed that the equation of state parameter gives quintessence-like nature of the universe in most of the cases. Also, the squared speed of sound shows stability of Tsallis and Rényi dark energy model but unstable behavior for Sharma-Mittal dark energy model. The $\omega_d - \omega_d'$ plane represents the thawing region for all dark energy models.

## 1. Introduction

In the last few years, remarkable progress has been achieved in the understanding of the universe expansion. It has been approved by current observational data that the universe undergoes an accelerated expansion. The observations of type Ia Supernovae (SNeIa)[1–4], large scale structure (LSS) [5–8], and Cosmic Microwave Background Radiation (CMBR) [9, 10] determined that the expansion of the universe is currently accelerating. There is also consensus that this acceleration is generally believed to be caused by a mysterious form of energy or exotic matter with negative pressure so called dark energy (DE) [11–21].

The discovery of accelerating expansion of the universe is a milestone for cosmology. It is considered that 95% of our universe is composed of two components, that is DE and dark matter [16]. The dark matter constitutes about 25% of the total energy density of the universe. The existence of the universe is proved by astrophysical observation but the nature of dark matter is still unknown. Mainly the DE is also a curious component of our universe. It is responsible for current accelerating universe and DE is entirely different from baryonic matter. DE constitutes almost 70% of the total energy density of our universe.

In order to describe the accelerated expansion phenomenon, two different approaches have been adopted. One is the proposal of various dynamical DE models such as family of Chaplygin gas, holographic dark energy, quintessence, K-essence, and ghost [16]. A second approach for understanding this strange component of the universe is modifying the standard theories of gravity, namely, general relativity (GR). Several modified theories of gravity are $f(R)$, $f(T)$ [17], $f(R, \mathrm{T})$ [18], and $f(G)$ [19], where $R$ is the curvature scalar, $T$ denotes the torsion scalar, T is the trace of the energy-momentum tensor, and $G$ is the invariant of Gauss-Bonnet.

Holographic DE (HDE) model is favorable technique to solve DE mystery which has attracted much attention and is based upon the holographic principle that states the number of degrees of freedom of a system scales with its area instead of its volume. In fact, HDE relates the energy density of quantum fields in vacuum (as the DE candidate) to the infrared and ultraviolet cut-offs. In addition, HDE is an interesting effort in exploring the nature of DE in the framework of quantum gravity. Cohen et al. [22] reported that the construction of HDE density is based on the relation with the vacuum energy of the system whose maximum amount should not exceed the black hole mass. Cosmological consequences of some HDE models in the dynamical Chern-Simons framework, as a modified gravity theory, can be found in [23].

By considering the long term gravity with the nature of spacetime, different entropy formalism has been used to observe the gravitational and cosmological effects [24–29]. The HDE models such as Tsallis HDE (THDE) [27], Rényi HDE model (RHDE) [28], and Sharma-Mittal HDE (SMHDE) [29] have been recently proposed. In the standard cosmology framework and from the classical stability view of point, while THDE is not stable [27], RHDE is stable during the cosmic evolution [28] and SMHDE is stable only whenever it becomes dominant in the world [29]. In the present work, we use the Tsallis, Sharma-Mittal, and Rényi entropies in the framework of dynamical Chern-Simons modified gravity and consider an interaction term. We investigate the different cosmological parameters such as equation of state parameter and the cosmological $\omega_d - \omega'_d$ plane where $\omega'_d$ shows the evaluation with respect to $\ln a$. We also investigate the squared sound speed of the HDE model to check the stability and the graphical approach.

This paper is organized as follows. In Section 2, we provide the basics of Chern-Simons modified gravity. In Section 3, we observe the equation of state parameter (EoS), cosmological plane, and squared sound speed for THDE model. Sections 4 and 5 are devoted to finding the cosmological parameter, cosmological plane, and squared of sound speed for RHDE and SMHDE models, respectively. In the last section, we conclude the results.

## 2. Dynamical Chern-Simons Modified Gravity

In this section, we give a review of dynamical Chern-Simons modified gravity. The action which describes the Chern-Simons modified gravity is given as

$$S = \frac{1}{16\pi G}\int_v d^4x \left[\sqrt{-g}R + \frac{l}{4}\theta^{*}R^{\rho\sigma\mu\nu}R_{\rho\sigma\mu\nu} - \frac{1}{2}g^{\mu\nu}\nabla_\mu\theta\nabla_\nu\theta + V(\theta)\right] + S_{mat}, \quad (1)$$

where $R$ represents the Ricci scalar, ${}^{*}R^{\rho\sigma\mu\nu}R_{\rho\sigma\mu\nu}$ is a topological invariant called the Pontryagin term, $l$ is a coupling constant, $\theta$ shows the dynamical variable, $S_{mat}$ represents the action of matter, and $V(\theta)$ is the potential term. In the case of string theory, we use $V(\theta) = 0$. By varying the action equation with respect to $g_{\mu\nu}$ and the scalar field $\theta$, we get the following field equations:

$$G_{\mu\nu} + lC_{\mu\nu} = 8\pi G T_{\mu\nu},$$
$$g^{\mu\nu}\nabla_\mu\nabla_\nu\theta = -\frac{l}{64\pi}{}^{*}R^{\rho\sigma\mu\nu}R_{\rho\sigma\mu\nu}. \quad (2)$$

Here, $G_{\mu\nu}$ and $C_{\mu\nu}$ are Einstein tensor and Cotton tensor, respectively. The Cotton tensor $C_{\mu\nu}$ is defined as

$$C_{\mu\nu} = -\frac{1}{2\sqrt{-g}}\left(\left(\nabla_\rho\theta\right)\varepsilon^{\rho\beta\tau(\mu}\nabla_\tau R^{\nu)}_\beta\right) + \left(\nabla_\sigma\nabla_\rho\theta\right){}^{*}R^{\rho(\mu\nu)\sigma}. \quad (3)$$

The energy-momentum tensor is given by

$$\hat{T}^{\theta}_{\mu\nu} = \nabla_\mu\theta\nabla_\nu\theta - \frac{1}{2}g_{\mu\nu}\nabla^\rho\theta\nabla_\rho\theta,$$
$$T_{\mu\nu} = (\rho + p)u_\mu u_\nu + pg_{\mu\nu}, \quad (4)$$

where $T_{\mu\nu}$ shows the matter contribution and $\hat{T}^{\theta}_{\mu\nu}$ represents the scalar field contribution, while $P$ and $\rho$ represent the pressure and energy density, respectively. Furthermore, $u_\mu = (1,0,0,0)$ is the four velocity. In the framework of Chern-Simons gravity, we get the following Friedmann equation:

$$H^2 = \frac{1}{3}(\rho_m + \rho_d) + \frac{1}{6}\dot{\theta}^2, \quad (5)$$

where $H = \dot{a}/a$ is the Hubble parameter and the dot represents the derivative of $a$ with respect to $t$ and $8\pi G = 1$. For FRW spacetime, the pony trying term ${}^{*}RR$ vanishes identically; therefore, the scalar field in (2) takes the following form:

$$g^{\mu\nu}\nabla_\mu\nabla_\nu\theta = g^{\mu\nu}\left[\partial_\nu\partial_\mu\theta\right] = 0. \quad (6)$$

We set $\theta = \theta(t)$ and get the following equation:

$$\ddot{\theta} + 3H\dot{\theta} = 0, \quad (7)$$

which implies that $\dot{\theta} = ba^{-3}$, $b$ is a constant of integration. Using this result in (5), we have

$$H^2 = \frac{1}{3}(\rho_m + \rho_d) + \frac{1}{6}b^2a^{-6}. \quad (8)$$

We consider the interacting scenario between DE and dark matter and thus equation of continuity turns to the following equations:

$$\dot{\rho}_m + 3H\rho_m = Q, \quad (9)$$

$$\dot{\rho}_d + 3H(\rho_d + p_d) = -Q. \quad (10)$$

Here, $\rho_d$ is the energy density of the DE, $\rho_m$ is the energy density of the pressureless matter, and $Q$ is the interaction term. Basically, $Q$ represents the rate of energy exchange between DE and dark matter. If $Q > 0$, it shows that energy is being transferred from DE to the dark matter. For $Q < 0$, the energy is being transferred from dark matter to the DE. We consider a specific form of interaction which is defined as $Q = 3Hd^2\rho_m$ and $d^2$ is interacting parameter which shows the energy transfers between CDM and DE. If we take $d = 0$, then it shows that each component, that is, the nonrelativistic matter and DE, is self-conserved. Using the value of $Q$ in (9) we have

$$\rho_m = \rho_{m0} a^{-3(1-d^2)}, \tag{11}$$

where $\rho_{m0}$ is an integration constant. Hence, (10) finally leads to the expression for pressure as follows:

$$p_d = -\left(d^2\rho_m + \rho_d + \frac{\dot{\rho}_d}{3H}\right), \tag{12}$$

The **EoS parameter** is used to categorize the decelerated and accelerated phases of the universe. This parameter is defined as

$$\omega = \frac{p}{\rho}. \tag{13}$$

If we take $\omega = 0$, it corresponds to nonrelativistic matter and the decelerated phase of the universe involves radiation era $0 < \omega < 1/3$. $\omega = -1, -1 < \omega < -1/3$, and $\omega < -1$ correspond to the cosmological constant, quintessence, and phantom eras respectively. To analyze the dynamical properties of the DE models, we use $\omega - \omega'$ **plane** [30]. This plane describes the evolutionary universe with two different cases, freezing region and thawing region. In the freezing region the values of EoS parameter and evolutionary parameter are negative ($\omega < 0$ and $\omega' < 0$), while for the thawing region, the value of EoS parameter is negative and evolutionary parameter is positive ($\omega < 0$ and $\omega' > 0$). In order to check the stability of the DE models, we need to evaluate the **squared sound speed** which is given by

$$v_s^2 = \frac{dp}{d\rho} = \frac{dp/dt}{d\rho/dt}. \tag{14}$$

The sign of $v_s^2$ decides its stability of DE models, when $v_s^2 > 0$, the model is stable; otherwise, it is unstable.

## 3. Tsallis Holographic Dark Energy

The definition and derivation of standard HDE density are given by $\rho_d = 3c^2{m_p}^2/L^2$, where ${m_p}^2$ represents reduced Plank mass and $L$ denotes the infrared cut-off. It depends upon the entropy area relationship of black holes, i.e., $S \sim A \sim L^2$, where $A = 4\pi L^2$ represents the area of the horizon. Tsallis and Cirto [31] showed that the horizon entropy of the black hole can be modified as

$$S_\delta = \gamma A^\delta, \tag{15}$$

where $\delta$ is the nonadditivity parameter and $\gamma$ is an unknown constant [31]. Cohen at al. [22] proposed the mutual relationship between IR (L) cut-off, system entropy (S), and UV ($\Lambda$) cut-off as

$$L^3\Lambda^3 \le (S)^{3/4}. \tag{16}$$

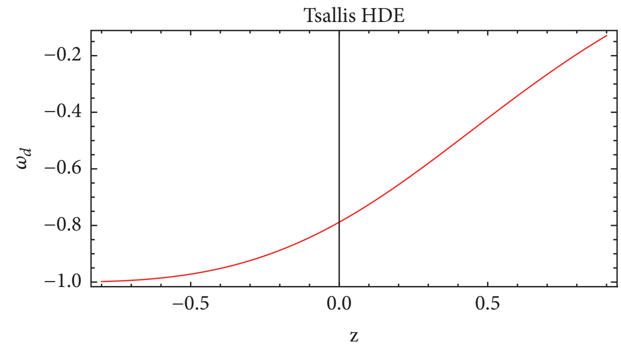


Figure 1: Plot of $\omega_d$ versus $z$ for THDE model where $\delta = 1.1$, $\rho_{m0} = 1$, $d^2 = 0.001$, $B = -1.3$, $b = 0.5$.

After combining (15) and (16), we get the following relation:

$$\Lambda^4 \le \gamma (4\pi)^\delta L^{2\delta-4}, \tag{17}$$

where $\Lambda^4$ is vacuum energy density and $\rho_d \sim \Lambda^4$. So, the Tsallis HDE density [29] is given as

$$\rho_d = BL^{2\delta-4}. \tag{18}$$

Here, $B$ is an unknown parameter and IR cut-off is taken as Hubble radius which leads to $L = 1/H$, where $H$ is Hubble parameter. The density of Tsallis HDE model along with its derivative by using (18) becomes

$$\begin{aligned} \rho_d &= BH^{4-2\delta}, \\ \dot{\rho}_d &= B(4-2\delta)H^{3-2\delta}\dot{H}. \end{aligned} \tag{19}$$

Here, $\dot{H}$ is the derivative of Hubble parameter w.r.t. $t$. The value of $\dot{H}$ is calculated in terms of $z$ using $a = 1/(1+z)$ which is given as follows.

$$\frac{dH}{dz} = \frac{(1/2)\left(\rho_{m0}\left(1-d^2\right)(1+z)^{3(1-d^2)} + b^2(1+z)^6\right)}{\left(1-(1/3)B(4-2\delta)H^{3-2\delta}\right)H(1+z)} \tag{20}$$

Inserting these values in (12) yields

$$\begin{aligned} p_d = \frac{1}{3}\Big(&-3d^2\rho_{m0}a^{-3(1-d^2)} \\ &- BH^{2-2\delta}\left(3H^2 + (4-2\delta)\dot{H}\right)\Big). \end{aligned} \tag{21}$$

The EoS is obtained from (13):

$$\omega_d = \frac{p_d}{\rho_d} = -1 - \frac{d^2\rho_{m0}a^{-3(1-d^2)}H^{2\delta-4}}{B} + \frac{(2\delta-4)\dot{H}}{3H^2}. \tag{22}$$

The plot of $\omega_d$ versus $z$ is shown in Figure 1. In this parameter and further results, the function $H(z)$ is being utilized numerically. The other constant parameters are mentioned

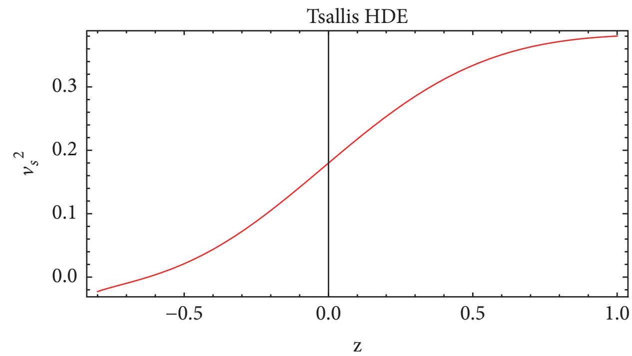


FIGURE 2: Plot of $v_s^2$ versus $z$ for THDE model where $\delta = 1.1$, $\rho_{m0} = 0.8$, $d^2 = 0.001$, $B = -1.3$, $b = 0.5$.

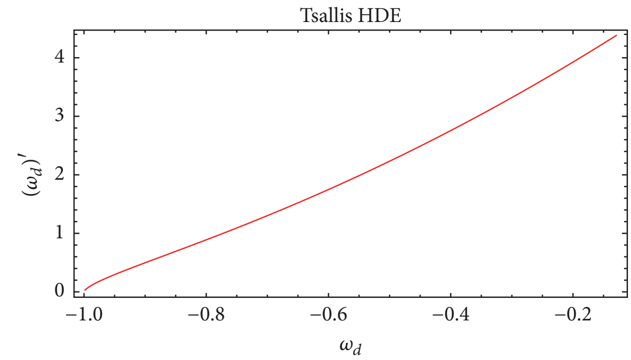


FIGURE 3: Plot of $\omega_d$ versus $\omega_d'$ for THDE model where $\delta = 1.1$, $\rho_{m0} = 1$, $d^2 = 0.001$, $B = -1.3$, $b = 0.5$.

in Figure 1. The trajectory of EoS parameter remains in quintessence region at early, present, and latter epoch.

The square of the sound speed is given by

$$v_s^2 = \frac{1}{6B(\delta-2)a^4H^3\dot{H}}\left(9d^2\left(d^2-1\right)\rho_{m0}a^{3d^2}H^{2\delta}\dot{a} - 2B(\delta-2)a^4H \times \left(3H^2\dot{H} - 2(\delta-1)\dot{H}^2 + H\ddot{H}\right)\right). \tag{23}$$

The plot of squared sound speed versus $z$ is shown in Figure 2 for different parametric values. This graph is used to analyze the stability of this model. We can see that $v_s^2 > 0$, for $-0.6 < z < 1$ which corresponds to the stability of THDE model. However, the model shows instability for $z < -0.6$.

Taking the derivative of the EoS parameter with respect to $\ln a$, we get $\omega_d'$ as follows.

$$\omega_d' = \frac{1}{3Ba^4H^6}\left(-3d^2\rho_{m0}^{3d^2}H^{2\delta}\left(3\left(d^2-1\right)H\dot{a} + (2\delta-4)\dot{H}\right) + 2B(\delta-2) \times a^4H^2\left(-2\dot{H}^2 + H\ddot{H}\right)\right) \tag{24}$$

The graph of $\omega_d$ versus $\omega_d'$ is shown in Figure 3, for which $\omega_d'$ depicts positive behavior. Hence, for $\omega_d < 0$, the evolution parameter shows $\omega_d' > 0$, which represents the thawing region of evolving universe.

## 4. Rényi Holographic Dark Energy Model

We consider a system with $W$ states with probability of getting $i^{\text{th}}$ state $P_i$ and satisfying the condition $\Sigma_{i=1}^{W}P_i = 1$. Rényi and Tsallis entropies are defined as

$$\mathcal{S} = \frac{1}{\delta}\ln\Sigma_{i=1}^{W}P_i^{1-\delta}, \qquad S_T = \frac{1}{\delta}\Sigma_{i=1}^{W}\left(P_i^{1-\delta} - P_i\right), \tag{25}$$

where $\delta \equiv 1-U$, where $U$ is a real parameter. Now, combining the above equations, we find their mutual relation given as

$$\mathcal{S} = \frac{1}{\delta}\ln\left(1 + \delta S_T\right). \tag{26}$$

This equation shows that $\mathcal{S}$ belongs to the class of most general entropy functions of homogenous system. Recently, it has been observed that Bekenstein entropy, $S = A/4$, is in fact Tsallis entropy which gives the expression

$$S = \frac{1}{\delta}\ln\left(1 + \delta\frac{A}{4}\right), \tag{27}$$

which is the Rényi entropy of the system. Now for the RHDE, we focus on WMAP data for flat universe. Using the assumption $\rho_d dv \propto T ds$, we can get RHDE density

$$\rho_d = \frac{3C^2H^2}{8\pi\left(1 + \delta\pi/H^2\right)}. \tag{28}$$

Considering the term $8\pi = 1$ and substituting in (28), we get the expression for density as

$$\rho_d = \frac{3C^2H^2}{1 + \delta\pi/H^2}. \tag{29}$$

Now, $dH/dz$ is given by the following.

$$\frac{dH}{dz} = \frac{(1/2)\left(\rho_{m0}\left(1-d^2\right)(1+z)^{3(1-d^2)} + b^2(1+z)^6\right)}{\left(1 - \left(2c^2H^2\left(z^2+\delta\pi\right) - c^2H^4\right)/\left(H^2+\delta\pi\right)^2\right)H(1+z)} \tag{30}$$

The pressure for this case is obtained as

$$p_d = -d^2\rho_{m0}a^{-3(1-d^2)} + \frac{c^2H^2\left(-3H^2\left(\pi\delta + H^2\right) - 2\left(2\pi\delta + H^2\right)\dot{H}\right)}{\left(\pi\delta + H^2\right)^2}. \tag{31}$$

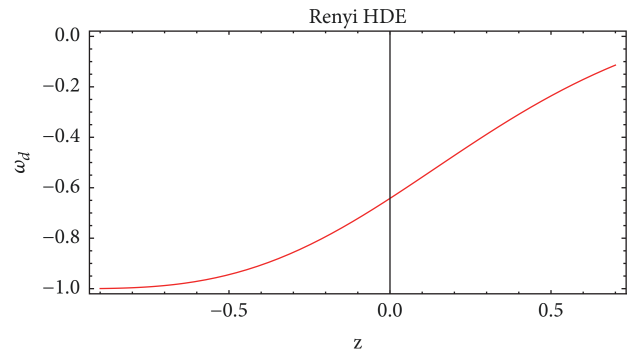


Figure 4: Plot of $\omega_d$ versus $z$ for RHDE model where $\delta = 1.1$, $\rho_{m0} = 0.8$, $d^2 = 0.001$, $c = 0.1$, $b = 0.05$.

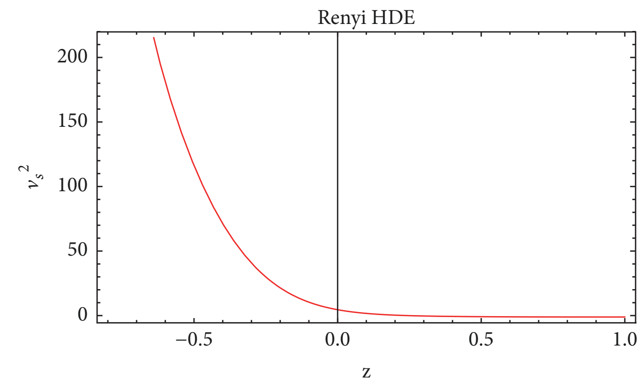


Figure 5: Plot of $v_s^2$ versus $z$, for RHDE model where $\delta = 1.1$, $\rho_{m0} = 0.8$, $d^2 = 0.001$, $c = 0.1$, $b = 1.5$.

The expressions for EoS parameter $\omega_d$ can be evaluated from (12) as follows:

$$\omega_d = \left(\pi\delta + H^2\right)\left(\frac{-d^2\rho_{m0}a^{-3(1-d^2)}}{3c^2H^4} - \frac{\left(3H^2\left(\pi\delta + H^2\right) + 2\left(2\pi\delta + H^2\right)\dot{H}\right)}{3H^2\left(\pi\delta + H^2\right)^2}\right). \tag{32}$$

Figure 4 shows the plot of $\omega_d$ versus $z$. The trajectory of EoS parameter evolutes the universe from quintessence region towards the ΛCDM limit. The squared sound speed of this RHDE model is given by using (13) as

$$\begin{aligned} v_s^{\,2} = {} & \frac{3H\left(1-d^2\right)d^2\rho_{m0}a^{-3(1-d^2)}\left(\pi\delta + H^2\right)^2}{6c^2H^3\left(2\pi\delta + H^2\right)\dot{H}} \\ & - \frac{1}{3H^2\left(2\pi\delta + H^2\right)\left(\pi\delta + H^2\right)} \\ & \times \left\{\dot{H}\left(6\pi^2\delta^2H^2 + 9\pi\delta H^4 + 3H^6 + 4\pi^2\delta^2\dot{H}\right)\right. \\ & \left. + H\ddot{H}\left(\pi\delta + H^2\right)\times\left(2\pi\delta + H^2\right)\right\}. \end{aligned} \tag{33}$$

The graph of squared speed of sound is shown in Figure 5 versus $z$. In this case, we have $v_s^2 > 0$ for all ranges of $z$, which shows the stability of RHDE model at the early, present, and latter epoch of the universe.

The expression for $\omega_d'$ is evaluated as

$$\begin{aligned} \omega_d' = {} & \frac{1}{3c^2a^4H^6\left(\pi\delta + H^2\right)^2}\left\{-d^2\rho_{m0}a^{3d^2}\left(\pi\delta + H^2\right)^2\right. \\ & \cdot\left(3H\dot{a}\left(-1 + d^2\right)\right. \\ & \left.\times\left(\pi\delta + H^2\right) - 2a\dot{H}\left(2\pi\delta + H^2\right)\right) \\ & + 2c^2a^4H^2\left(4\pi^2\delta^2 + 8\pi\delta H^2 + 2H^4\right)\dot{H}^2 - 2H\left(\pi\delta\right. \\ & \left.\left. + H^2\right)\left(2\pi\delta + H^2\right)\ddot{H}\right\}. \end{aligned} \tag{34}$$

In Figure 6, we plot the EoS parameter with its evolution parameter to discuss $\omega_d - \omega_d'$ plane for RHDE model. The graph shows that, for $\omega_d < 0$, the evolutionary parameter remains positive at the early, present, and latter epoch. This type of behavior depicts the thawing region of the evolving universe.

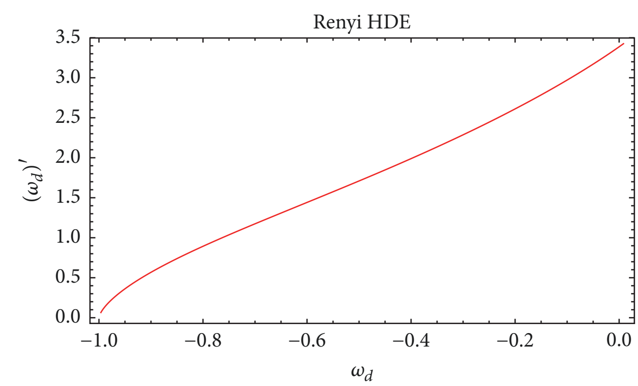


Figure 6: Plot of $\omega_d$ versus $\omega_d'$ for RHDE model where $\delta = 1.1$, $\rho_{m0} = 0.8$, $d^2 = 0.001$, $c = 0.1$, $b = 0.05$.

## 5. Sharma-Mittal Holographic Dark Energy Model

From the Rényi entropy, we have the generalized entropy content of the system. Using (26), Sharma-Mittal introduced a two-parametric entropy which is defined as

$$S_{SM} = \frac{1}{1-r}\left(\left(\Sigma_{i=1}^{W}P_i^{1-\delta}\right)^{1-r/\delta} - 1\right), \tag{35}$$

where $r$ is a new free parameter. We can observe that Rényi and Tsallis entropies can be recovered at the proper limits; using (25) in (35), we have

$$S_{SM} = \frac{1}{R}\left(\left(1 + \delta S_T\right)^{R/\delta} - 1\right), \tag{36}$$

where $R \equiv 1-r$. Using the argument that Bekenstein entropy is the proper candidate for Tsallis entropy by using $S = A/4$, where $A$ is horizon entropy, we get the following expression:

$$S_{SM} = \frac{1}{R}\left(\left(1+\delta\frac{A}{4}\right)^{R/\delta} - 1\right), \quad (37)$$

and the relation of UV ($\Lambda$) cut-off, IR (L) cut-off, and system horizon (S) is given as follows.

$$\Lambda^4 \propto \frac{S}{L^4} \quad (38)$$

Now, taking $L \equiv 1/H = \sqrt{A/4\pi}$, then the energy density of DE given by Sharma-Mittal [29] is considered as

$$\rho_d = \frac{3c^2H^4}{8\pi R}\left[\left(1+\frac{\delta\pi}{H^2}\right)^{R/\delta} - 1\right], \quad (39)$$

where $c^2$ is an unknown free parameter. Using $8\pi = 1$ in above equation, we get the following expression for energy density

$$\rho_d = \frac{3c^2H^4}{R}\left[\left(1+\frac{\delta\pi}{H^2}\right)^{R/\delta} - 1\right]. \quad (40)$$

The differential equation of $H$ is given by the following.

$$\frac{dH}{dz} = \frac{(1/2)\left(\rho_{m0}\left(1-d^2\right)(1+z)^{3(1-d^2)} + b^2(1+z)^6\right)}{1 + c^2\pi\left(1+(\delta\pi/H^2)\right)^{R/\delta-1} - \left(2c^2H^2/R\right)\left(\left(1+\delta\pi/H^2\right)^{R/\delta} - 1\right)H(1+z)} \quad (41)$$

The pressure can be evaluated by energy conservation (11) as follows:

$$\begin{aligned} p_d = {} & -d^2\rho_{m0}a^{-3(1-d^2)} \\ & - c^2\left(\frac{3\left(\left(1+\pi\delta/H^2\right)^{R/\delta} - 1\right)H^4}{R}\right. \\ & - 2\pi\dot{H}\left(1+\frac{\pi\delta}{H^2}\right)^{R/\delta-1} \\ & \left. + \frac{4\left(\left(1+\pi\delta/H^2\right)^{R/\delta} - 1\right)H^2\dot{H}}{R}\right). \end{aligned} \quad (42)$$

The EoS parameter for this model is given by

$$\begin{aligned} \omega_d = {} & 2c^2\left(\pi\left(1+\frac{\pi\delta}{H^2}\right)^{R/\delta-1}\right. \\ & \left. - \frac{2H^2\dot{H}}{R}\left(\left(1+\frac{\pi\delta}{H^2} - 1\right)^{R/\delta}\right)\right) \\ & - \frac{d^2R\rho_{m0}a^{-3(1-d^2)}}{3c^2H^4\left(\left(1+\delta\pi/H^2\right)^{R/\delta} - 1\right)} - 1. \end{aligned} \quad (43)$$

The plot of $\omega_d$ versus $z$ is shown in Figure 7. The EoS parameter represents the quintessence nature of the universe. The square of the sound speed is evaluated as

$$\begin{aligned} v_s^2 = {} & \frac{1}{6c^2H\dot{H}\left(-\pi\left(1+\pi\delta/H^2\right)^{R/\delta-1} + \left(2H^2/R\right)\left(\left(1+\pi\delta/H^2\right)^{R/\delta} - 1\right)\right)} \times \left\{-3d^2H\left(-1+d^2\right)\rho_{m0}a^{-3(1-d^2)}\right. \\ & + \frac{2c^2H}{R}\left(6H^2\dot{H} + 4\dot{H}^2 + 2H\ddot{H} - \frac{1}{\left(\pi\delta+H^2\right)^2}\left(1+\frac{\pi\delta}{H^2}\right)^{R/\delta}\right. \\ & \cdot\left(3H^2\dot{H}\left(\pi\delta+H^2\right)\left(-\pi R + 2\pi\delta + 2H^2\right) + 2\dot{H}\left(\pi^2(R-2\delta)(R-\delta) - 2\dot{H}^2\pi(R-2\delta)H^2 + 2H^4\right)\right) \\ & \left.\left. + H\dot{H}\left(\pi\delta+H^2\right)\times\left(-\pi R + 2\pi\delta + 2H^2\right)\ddot{H}\right)\right\}. \end{aligned} \quad (44)$$

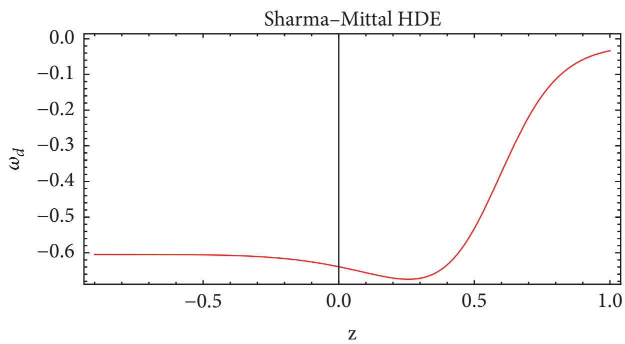


Figure 7: Plot of $\omega_d$ versus $z$ for SMHDE where $\delta = 1.1$, $\rho_{m0} = 0.01$, $d^2 = 0.001$, $c = 0.01$, $b = 0.4$, $R = 7$.

In Figure 8, we draw $v_s^2$ versus $z$ which shows the unstable behavior of the SMHDE model as $v_s^2 < 0$ at early, present, and latter epoch.

$$\begin{aligned}
\omega_d' = & -\frac{1}{3\left(\left(1+\pi\delta/H^2\right)^{R/\delta}-1\right)^2 H^6}\bigg(\frac{1}{\left(\pi\delta+H^2\right)^2} \\
& \cdot 2H^2\bigg(2\bigg(-2\left(\pi\delta+H^2\right)^2+\left(1+\frac{\pi\delta}{H^2}\right)^{2R/\delta} \\
& \cdot\left(\pi^2\left(R-2\delta\right)\delta+2\pi\left(R-2\delta\right)H^2-2H^4\right) \\
& +\left(1+\frac{\pi\delta}{H^2}\right)^{R/\delta} \\
& \times\left(-\pi^2\left(R^2+R\delta-4\delta^2\right)-2\pi\left(R-4\delta\right)H^2+4H^4\right)\bigg) \\
& \cdot\dot{H}^2+\left(\pi\delta+H^2\right)\times\left(\left(1+\frac{\pi\delta}{H^2}\right)^{R/\delta}-1\right) \\
& \cdot H\bigg(-2\left(\pi\delta+H^2\right)+\left(1+\frac{\pi\delta}{H^2}\right)^{R/\delta} \\
& \times\left(-\pi R+2\pi\delta+2H^2\right)\bigg)\ddot{H}\bigg)+\frac{3d^2\left(-1+d^2\right)}{c^2} \\
& \cdot\rho_{m0}Ra^{-3(1-d^2)}H^2\times\left(\left(1+\frac{\pi\delta}{H^2}\right)^{R/\delta}-1\right) \\
& +\frac{2d^2\rho_{m0}Ra^{-3(1-d^2)}}{c^2\left(\pi\delta+H^2\right)}\bigg(\left(\pi\left(R-2\delta\right)-2H^2\right)\times\bigg(1 \\
& +\frac{\pi\delta}{H^2}\bigg)^{R/\delta}+2\left(\pi\delta+H^2\right)\bigg)\dot{H}\bigg)
\end{aligned} \tag{45}$$

Figure 9 shows the plot of $\omega_d$-$\omega_d'$ plane to classify the dynamical region for the given model. We can see that $\omega_d' > 0$ for $\omega_d < 0$, which indicates the thawing region of the universe.

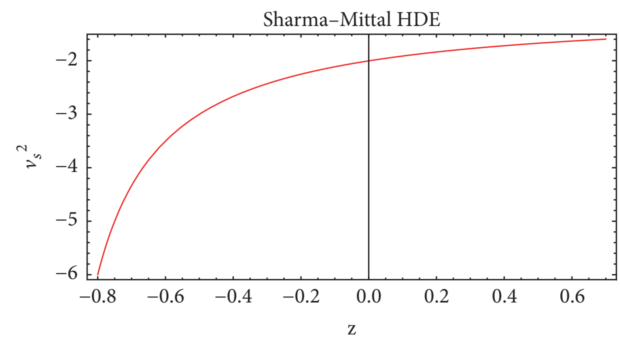


Figure 8: Plot of $v_s^2$ versus $z$ for SMHDE where $\delta = 1.1$, $\rho_{m0} = 0.8$, $d^2 = 0.001$, $c = 0.8$, $b = 0.05$, $R = 7$.

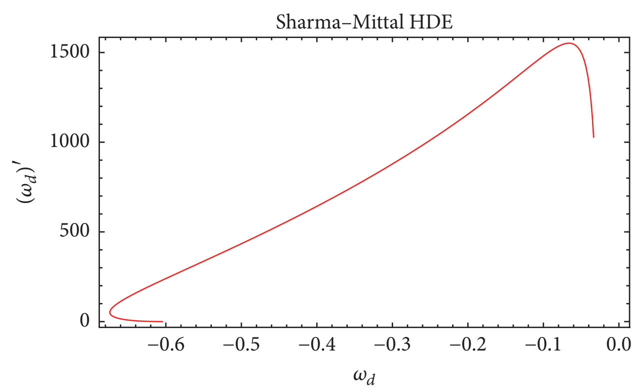


Figure 9: Plot of $\omega_d$ versus $\omega_d'$ for different values of $\delta$ for SMHDE where $\delta = 1.1$, $\rho_{m0} = 0.01$, $d^2 = 0.001$, $c = 0.01$, $b = 0.4$, $R = 7$.

Table 1: Summary of the cosmological parameters and plane.

| DE models | $\omega_d$ | $v_s^2$ | $\omega_d - \omega_d'$ |
|---|---|---|---|
| THDE | quintessence-to-vacuum | partially stability | thawing region |
| RHDE | quintessence-to-vacuum | stability | thawing region |
| SMHDE | quintessence | un-stable | thawing region |

## 6. Conclusion

In this paper, we have discussed the THDE, RHDE, and SMHDE models in the framework of Chern-Simons modified theory of gravity. We have taken the flat FRW universe, and linear interaction term is chosen for the interacting scenario between DE and dark matter. We have evaluated the different cosmological parameters (equation of state parameter and squared sound speed), $\omega_d - \omega_d'$ cosmological plane. The trajectories of all these models have been plotted with different constant parametric values.

We have summarized our results in Table 1.

Jawad et al. [32] have explored various cosmological parameters (equation of state, squared speed of sound, Om-diagnostic) and cosmological planes in the framework of dynamical Chern-Simons modified gravity with the new holographic dark energy model. They observed that the equation of state parameter gives consistent ranges by using different observational schemes. They also found that the squared speed of sound shows a stable solution. They suggested that the results of cosmological parameters show consistency with recent observational data. Jawad et al. [33] have also considered the power law and the entropy corrected HDE models with Hubble horizon in the dynamical Chern-Simons modified gravity. They have also explored various cosmological parameters and planes and found consistent results with observational data. Nadeem et al. [34] have also investigated the interacting modified QCD ghost DE and generalized ghost pilgrim DE with cold dark matter in the framework of dynamical Chern-Simons modified gravity. It is found that the results of cosmological parameters as well as planes explain the accelerated expansion of the universe and are compatible with observational data.

However, the present work is different from the above-mentioned works in which we have recently proposed DE models along with nonlinear interaction term and found interesting and compatible results regarding current accelerated expansion of the universe.

## Data Availability

The data used to support the findings of this study are available from the corresponding author upon request.

## Conflicts of Interest

The authors declare that there are no conflicts of interest regarding the publication of this paper.

## Acknowledgments

The work of H. Moradpour has been supported financially by Research Institute for Astronomy & Astrophysics of Maragha (RIAAM) under research project No. $1/5237-8$.

## References

[1] A. G. Riess, "Observational evidence from supernovae for an accelerating universe and a cosmological constant," *The Astronomical Journal*, vol. 116, 1998.

[2] S. Perlmutter, G. Aldering, G. Goldhaber et al., "Measurements of Ω and Λ from 42 High-Redshift Supernovae," *The Astrophysical Journal*, vol. 517, no. 2, pp. 565–586, 1999.

[3] P. de Bernardis, P. A. R. Ade, and J. J. Bock, "A flat Universe from high-resolution maps of the cosmic microwave background radiation," *Nature*, vol. 404, pp. 955–959, 2000.

[4] S. Perlmutter et al., "New constraints on ΩM, ΩΛ, and w from an independent set of 11 high-redshift supernovae observed with the hubble space telescope," *The Astrophysical Journal*, vol. 598, 2003.

[5] M. Colless et al., "The 2dF galaxy redshift survey: luminosity dependence of galaxy clustering," *Monthly Notices of the Royal Astronomical Society*, vol. 328, 2001.

[6] M. Tegmark et al., "Cosmological parameters from SDSS and WMAP," *Physical Review D*, vol. 69, Article ID 103501, 2004.

[7] S. Cole, "The 2dF galaxy redshift survey: power-spectrum analysis of the final data set and cosmological implications," *Monthly Notices of the Royal Astronomical Society*, vol. 362, 2005.

[8] V. Springel, C. S. Frenk, and S. D. M. White, "The large-scale structure of the Universe," *Nature*, vol. 440, no. 7088, pp. 1137–1144, 2006.

[9] C. B. Netterfeld, P. A. R. Ade, and J. J. Bock, "A measurement by BOOMERANG of multiple peaks in the angular power spectrum of the cosmic microwave background," *The Astrophysical Journal*, vol. 571, no. 2, pp. 604–614, 2002.

[10] D. N. Spergel et al., "First-year wilkinson microwave anisotropy probe (WMAP)$^*$ observations: determination of cosmological parameters," *The Astrophysical Journal Supplement Series*, vol. 148, 2003.

[11] T. Chiba, T. Okabe, and M. Yamaguchi, "Kinetically driven quintessence," *Physical Review D: Particles, Fields, Gravitation and Cosmology*, vol. 62, Article ID 023511, 2000.

[12] T. M. Aliev, M. Savcı, and B. B. Şirvanlı, "Double-lepton polarization asymmetries in $\Lambda_b \longrightarrow \Lambda\ell^+\ell^-$- decay in universal extra dimension model," *The European Physical Journal C*, vol. 52, no. 2, pp. 375–382, 2007.

[13] G. Pérez-Nadal, "Stability of de Sitter spacetime under isotropic perturbations in semiclassical gravity," *Physical Review D: Particles, Fields, Gravitation and Cosmology*, vol. 77, Article ID 124033, 2008.

[14] S. D. H. Hsu, "Entropy bounds and dark energy," *Physics Letters B*, vol. 594, no. 1-2, pp. 13–16, 2004.

[15] S. P. de Alwis, "Brane worlds in 5D and warped compactifications in IIB," *Physics Letters. B. Particle Physics, Nuclear Physics and Cosmology*, vol. 603, no. 3-4, pp. 230–238, 2004.

[16] K. Bamba, S. Capozziello, S. Nojiri, S. D. Odintsov, and K. Bamba, "Dark energy cosmology: the equivalent description via different theoretical models and cosmography tests," *Astrophysics and Space Science*, vol. 342, no. 1, pp. 155–228, 2012.

[17] W. A. Ponce, J. B. Flórez, and L. A. Sánchez, "Analysis of $SU(3)_c \times SU(3)_L \times U(1)_X$ local Gauge theory," *International Journal of Modern Physics A*, vol. 17, p. 643, 2002.

[18] E. H. Baffou, M. J. S. Houndjo, and J. Tossa, "Exploring stable models in $f(R;T;R_{\mu\nu};T^{\mu\nu})$ gravity," *Astrophysics and Space Science*, vol. 361, article 376, 2016.

[19] S. Nojiri and S. D. Odintsov, "Modified gauss-bonnet theory as gravitational alternative for dark energy," *Physics Letters B*, p. 1, 2005.

[20] M. Roos, *Introduction to Cosmology*, John Wiley and Sons, UK, 2003.

[21] S. Nojiri and S. D. Odintsov, "The new form of the equation of state for dark energy fluid and accelerating universe," *Physics Letters B*, vol. 639, no. 3-4, pp. 144–150, 2006.

[22] A. G. Cohen et al., "Effective field theory, black holes, and the cosmological constant," *Physical Review Letters*, vol. 82, pp. 4971–4974, 1999.

[23] A. Pasqua, R. da Rocha, and S. Chattopadhyay, "Holographic dark energy models and higher order generalizations in dynamical Chern-Simons modified gravity," *The European Physical Journal C*, vol. 75, article 44, 2015.

[24] H. Moradpour, A. Sheykhi, C. Corda, and I. G. Salako, "Implications of the generalized entropy formalisms on the Newtonian gravity and dynamics," *Physics Letters B*, vol. 783, pp. 82–85, 2018.

[25] H. Moradpour, A. Bonilla, E. M. C. Abreu, and J. A. Neto, "Accelerated cosmos in a nonextensive setup," *Physical Review D*, vol. 96, Article ID 123504, 2017.

[26] H. Moradpour, "Implications, consequences and interpretations of generalized entropy in the cosmological setups," *International Journal of Theoretical Physics*, vol. 55, no. 9, pp. 4176–4184, 2016.

[27] M. Tavayef, A. Sheykhi, K. Bamba, and H. Moradpour, "Tsallis holographic dark energy," *Physics Letters B*, vol. 781, pp. 195–200, 2018.

[28] H. Moradpour et al., "Thermodynamic approach to holographic dark energy and the Rényi entropy," *General Physics*, 2018.

[29] A. Sayahian Jahromi, S. A. Moosavi, H. Moradpour et al., "Generalized entropy formalism and a new holographic dark energy model," *Physics Letters. B. Particle Physics, Nuclear Physics and Cosmology*, vol. 780, pp. 21–24, 2018.

[30] E. J. Copeland, M. Sami, and S. Tsujikawa, "Dynamics of dark energy," *International Journal of Modern Physics D: Gravitation, Astrophysics, Cosmology*, vol. 15, no. 11, pp. 1753–1935, 2006.

[31] C. Tsallis and L. J. L. Cirto, "Black hole thermodynamical entropy," *The European Physical Journal C*, vol. 73, no. 7, p. 2487, 2013.

[32] A. Jawad, S. Rani, and T. Nawaz, "Interacting new holographic dark energy in dynamical Chern-Simons modified gravity," *The European Physical Journal Plus*, vol. 131, p. 282, 2016.

[33] A. Jawad, S. Rani, and N. Azhar, "Entropy corrected holographic dark energy models in modified gravity," *International Journal of Modern Physics D*, vol. 26, Article ID 1750040, 2016.

[34] N. Azhar, "Cosmological implications of dark energy models in modified gravity," *International Journal of Geometric Methods in Modern Physics*, vol. 15, Article ID 1850034, 2018.